Physicochemical model for simulating the chemical processes during the crystallization of minerals from spent ion exchange regenerant

Boncz, Marc Arpad; Van Linden, Niels; Haidari, Amir; Wang, Yundan; Spanjers, Henri

DOI
10.1016/j.wri.2022.100185

Publication date
2022

Document Version
Final published version

Published in
Water Resources and Industry

Water Resources and Industry 28 (2022) 100185

Contents lists available at ScienceDirect

Water Resources and Industry

journal homepage: www.elsevier.com/locate/wri

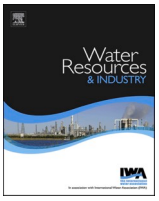

Physicochemical model for simulating the chemical processes during the crystallization of minerals from spent ion exchange regenerant

Marc Arpad Boncz [a,b,*], Niels van Linden [a], Amir Haidari [a], Yundan Wang [a], Henri Spanjers [a]

[a] Delft University of Technology, Faculty of Civil Engineering and Geosciences, Stevinweg 1, 2628 CN, Delft, the Netherlands
[b] Federal University of Mato Grosso Do Sul, Faculty of Architecture, Engineering, and Geography, Av. Costa e Silva S/N, 79070-900, Campo Grande-MS, Brazil

ARTICLE INFO

Keywords:
Brines
Sequential crystallisation
PHREEQC
Closed cycle
Metal recovery

ABSTRACT

Traditionally, industrial processes produce wastes that, even though often containing useful materials, are discarded, contributing to environmental pollution and depletion of natural resources. An example of such wastes are brines, flows of concentrated salts, produced in water treatment processes, which are now routinely discharged into receiving water bodies. Brines however can also be considered as flows of reusable materials which should be recovered, and the Zero Brine cooperation project aims to develop processes for that purpose. For a demineralized water production plant in the port of Rotterdam (the Netherlands), a closed water processing cycle was proposed to treat the large volume of spent Ion Exchange (IEX) regenerant brine which, apart from recovering demineralized water, is also intended to produce magnesium (Mg^{2+}) and calcium (Ca^{2+}) salts, with the highest purity possible, from the otherwise discharged brine. The process scheme includes nanofiltration (NF) for separating mono- and multivalent ions, followed by sequential chemical precipitation of Mg^{2+} and Ca^{2+} ions from the NF concentrate, and production of demineralized water by evaporation of the NF permeate. The concentrate of monovalent ions produced in the evaporator, essentially a concentrated sodium chloride solution, in its turn might be reused for IEX regeneration. Part of the supernatant of the sequential precipitation may be fed to the evaporator as well, but bleeding the other part of this supernatant is essential in order to maintain process stability, avoid accumulation of minor pollutants, and reduce scaling. In this study, various scenarios to operate the process were modeled, using PHREEQC and Excel. According to the simulation results, recovery of ≈97% of Mg^{2+} and Ca^{2+} is possible, the latter with a higher purity than the former. The main factors affecting the results are the concentration of carbonate present in the spent IEX regenerant, as well as characteristics of the NF membrane and the dosing of sodium hydroxide in the sequential precipitation steps. The results of the simulations were used for the design and operation of a pilot plant, comprising all mentioned process steps.

* Corresponding author. Federal University of Mato Grosso Do Sul, Faculty of Architecture, Engineering, and Geography, Av. Costa e Silva S/N, 79070-900, Campo Grande-MS, Brazil.
E-mail address: marc.boncz@ufms.br (M.A. Boncz).

https://doi.org/10.1016/j.wri.2022.100185
Received 8 November 2021; Received in revised form 14 July 2022; Accepted 20 July 2022
Available online 31 July 2022

1. Introduction

The Botlek is an industrial district of the port of Rotterdam (the Netherlands), with plants of a variety of large chemical companies, as well as transshipping facilities. Demineralized water is an essential commodity here because it is required for many production processes. Reverse osmosis (RO) has become one of the main processes for producing demineralized water, but RO alone is not enough to produce water of the required purity from the available water (fresh surface water), and several pre- and post-treatment processes are used, like for instance ion-exchange softening (IEX) [1].

At the demineralized water plant chosen for the demonstration project described here, demineralized water is produced from surface water withdrawn from the Brielse Meer (the Netherlands). This water is pretreated by means of coagulation/flocculation, dissolved air flotation (DAF), and filtration, before entering the actual demineralized water plant. The pretreated water has the same ion strength as the surface water, but may contain a low residual concentration of Fe(III), as $FeCl_3$ is used as coagulant. The IEX softening unit (unit A in Fig. 2, in the Materials and Methods section) removes bivalent cations like calcium (Ca^{2+}) and magnesium (Mg^{2+}), amongst others, substituting them for Na^{+} ions. The reverse osmosis (RO) unit (unit B) then separates the softened feed water into a permeate (flow 14) and a concentrate stream (flow 05). This concentrate, that will be disposed of in most cases, includes most of the ions of the feed water, but at higher concentrations, and with part of the cations substituted for Na^{+} ions. It also contains small amounts of residual dissolved organic pollutants. The permeate (flow 14), although essentially almost pure water, still contains low concentrations of monovalent salts and is, therefore, still not suitable to be distributed as demineralized water [2,3]. Typically, polishing steps are used to remove the trace of salts in this permeate to make it suitable to be used as demineralized water. As indicated, IEX softening is used as one of the pretreatment steps before RO to remove bivalent ions and enhance the recovery of RO. Frequent regeneration of the IEX resin is an essential procedure to maintain the required efficiency of this process. In this plant, regenerating the IEX resin occurs daily, by counter-current passing of a concentrated salt solution (NaCl brine), and the effluent from this IEX regenerating contains valuable ions such as Mg^{2+} and Ca^{2+}, amongst others. Disposing of the IEX regeneration solution could be costly and harmful to the environment.

Zero Brine is a cooperation project run with support of the European Union, and its main aim is to stimulate the development of technologies to treat brines that otherwise would be discharged into the environment, and recover valuable minerals and salts as well as water from these flows. At the demineralized water plant under study, aim is to treat the regeneration solution of the IEX unit (spent regenerant) and to recover water and Mg and Ca salts, using several technologies, including nanofiltration (NF), sequential crystallization and evaporation, as shown in Fig. 2. To begin, the NF installation will produce a NaCl rich solution with a NaCl purity of around 96% as its permeate (06), by rejecting a major part of the multivalent ions present in the regenerant solution. The NF concentrate will then be a concentrated solution of salts of mainly multivalent ions. The operation of this NF process has been studied before [4,5]. The characteristics of the permeate depend on parameters like permeate and reject flows, and reject percentages of different ions, which depend on the membrane used, amongst others. Recovery of the metal ions from the NF reject flow should then be possible by precipitating their low solubility sulphates, carbonates, or hydroxides, as represented by thin dotted, solid, and thick dotted lines respectively in Fig. 1. The least soluble compound is $CaMg(CO_3)_2$, dolomite, but precipitating this compound will not lead to separation of Mg and Ca and should thus be avoided, by keeping the (bi)carbonate concentration in the crystallization reactor as low as possible. Fortunately, dolomite precipitation is a very slow process, due to it being a reaction with third-order kinetics and a high energy of activation, and will not occur under normal conditions [6]. The second least soluble compound however is brucite, $Mg(OH)_2$, of which the solubility (thick dotted line, closed markers) differs greatly from that of portlandite (lime), $Ca(OH)_2$, (thinner dotted line, open markers), and thus permits sequential precipitation. Sequential crystallization of the sulphates should also be possible, but these

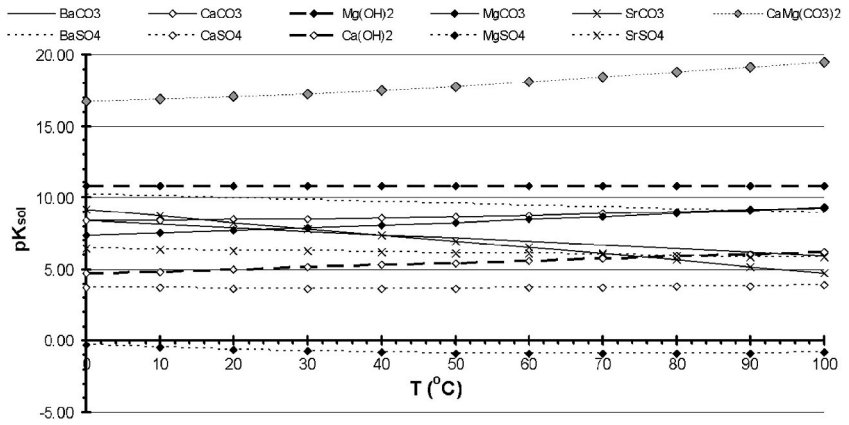

Fig. 1. Negative logarithms of solubility products ($pK_{sol} = -\log(K_{sp})$) of a number of salts of bivalent cations and carbonate, sulphate, or hydroxide [7]. Least soluble is $CaMg(CO_3)_2$ (dolomite, essentially insoluble at 25 °C), most soluble is $MgSO_4$ (solubility approx. 351 g L^{-1} at 25 °C). $Mg(OH)_2$ and $Ca(OH)_2$ are identified with thicker dotted lines and closed and open markers, respectively (identical cations always use the same marker, identical anions always the same line style). Relative solubilities depend on temperature, as the solubility of some minerals increases but of other minerals decreases with temperature.

are much more soluble, and sulphate would remain in the supernatant, making this a less suitable option. Interference may result from the low solubilities of several carbonates (solid lines, marker depends on cation). The NF concentrate will thus pass through a two-stage crystallization process. In the first stage, magnesium, and in the second stage, calcium will be recovered as metal hydroxides, by slowly dosing stoichiometric amounts of NaOH. To avoid contamination of the produced $Mg(OH)_2$ and $Ca(OH)_2$, the concentration of hydroxide ions but also of other anions will be shown to be of importance.

The joined NF permeate, essentially a slightly polluted NaCl brine, and the membrane crystallization supernatant will then be treated with an evaporator. In the evaporator, the solution will be separated into a condensate, essentially distilled water, and a solution with a high salinity. The condensate of the evaporator will be virtually free of any ions and can be used as demineralized water which is needed as well for the regeneration of the IEX columns. The high salinity brine will contain mostly NaCl, and might thus be used for regeneration of the IEX columns but, depending on conditions, unlimited recycling of the supernatant may deem this brine too polluted with other cations. This study has thus two objectives. First objective is to quantify sequential precipitation of magnesium and calcium hydroxides and the expected purity of the product. Second objective is to analyze the consequences and (im)possibility of recycling of the supernatant. In order to do so, the chemical reactions that are expected to take place during passing of the spent regenerant through the different processes are quantified using a solubility-constant based computer model (PHREEQC), developed by the USGS [8,9].

2. Material and methods

2.1. Data acquisition

The data used as a starting point for the modeling were determined from two sampling campaigns at a large Demineralized Water Plant in the port of Rotterdam, the Netherlands. Samples were taken in December 2017, and in March 2018, after each ion-exchange column, to determine not only the average concentrations of the individual ions, but also the effect of operating time of the ion exchange resin on the presence of secondary pollutants (cations other than H^+, Na^+, Ca^{2+} and Mg^{2+}). The samples were stored at 4 °C and analyzed at the Delft University of Technology water laboratory using ICP-MS (Plasma Quant MS, Analytik Jena, Germany) for the cations, and IC (Metrohm 881-IC, Metrohm, Switzerland, equipped with a Supp 5150/4.0 column) for the anions, using standard procedures. Bicarbonate, not measured by IC, was determined by titration of samples with 0.100 M HCl until a pH of 4.30 using a Metrohm 702SM Titrino automatic titrator. Temperature was determined on-site and pH was measured in the samples by means of a hand-held pH meter (WTW Multi 3410). Total Dissolved Solids (TDS) were determined gravimetrically.

2.2. Process scheme

Demineralized water is produced in the plant by means of a sequence of processes, including DAF, IEX and RO, the latter indicated as A and B in Fig. 2. Periodically, the IEX columns are regenerated, using a concentrated NaCl brine (flow 03), and this results in a flow of spent IEX regenerant (flow 04). Objective of the Zero Brine project is recovery of the salts and water from this flow, for which the additional process steps C to F (Fig. 2) are planned.

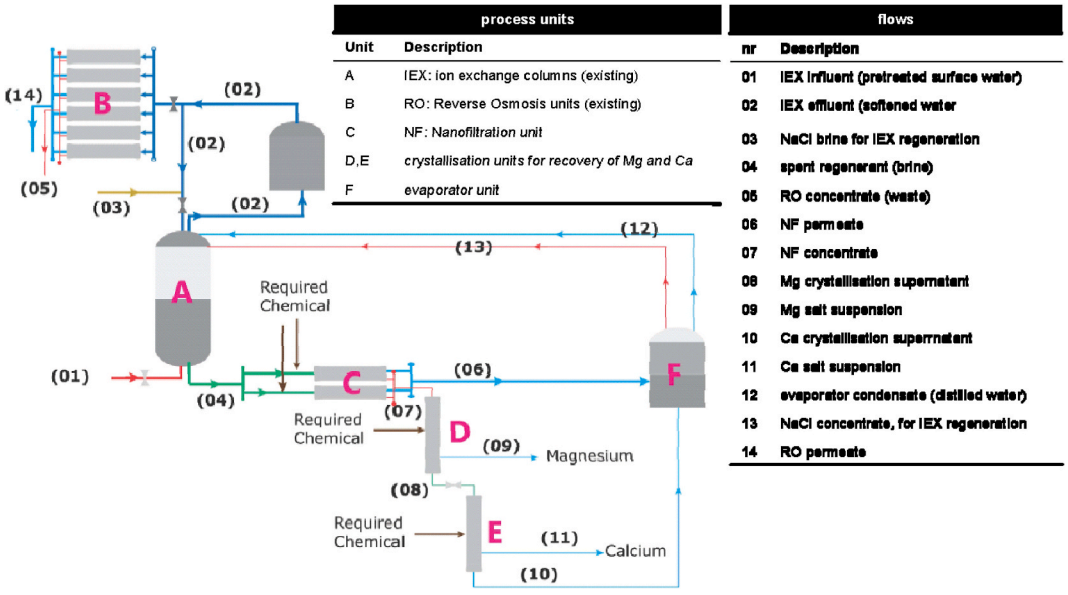

Fig. 2. Process flow diagram of the Zero Brine project for the Demineralized Water Plant, showing existing units (A&B) and new process units for salts and water recovery (C...F).

Process unit C is a NF unit, intended to reject bivalent anions and cations. Experiments were performed by the supplier of the NF membranes prior to modeling the process flow, and given the results of these experiments, rejections of 46%–80% for mono- and bivalent anions and of 30%–60% for mono- and bivalent cations were assumed, at a 70% recovery. The assumptions regarding the NF performance, as used in the modeling, are presented in Table 1:

As a result of this, the permeate flow (06) is basically a flow of concentrated NaCl, whereas the multivalent ions present in the spent IEX regenerant are concentrated in the reject flow (flow 07). These ions include the Mg^{2+} and Ca^{2+} ions, which are then to be precipitated in the crystallization units D and E, respectively. After crystallization of Mg and Ca salts in units D and E, the supernatant can either be discarded, or recycled to the evaporator F, which produces distilled (pure) water and a brine containing mainly NaCl.

2.3. Modeling

The calculations concerning the chemical reactions were performed using Excel, for making initial estimations of flows and rejects, and using PHREEQC Interactive 3.4.0, for detailed calculations of chemical equilibria and solubility and precipitation/crystallization. PHREEQC is a modeling program developed by the USGS [8,10], which has several databases, including solubility products of different groups of minerals, which are used for determining speciation of elements involved in the system under different conditions. Given the species present in the brine and expected to be relevant, the Minteq v.4 database (that can be found among the databases provided with PHREEQC Interactive 3.4.0) was used rather than the smaller Pitzer or PHREEQC generic databases, because it contains most measured elements.

The input values used for the PHREEQC simulations were not exactly the values obtained during the data-acquisition phase. For practical reasons, the following simplifications were made:

1. To simplify simulations, elements with concentrations $<1\ \mu g\ L^{-1}$ were neglected, which can be justified as salt concentrations in the samples were close to $30\ g\ L^{-1}$;
2. Cobalt (Co) and molybdenum (Mo) were not included in PHREEQC's Minteq database, and were therefore excluded from the simulations;
3. Notably, for both samples, the concentration of sulphur (S) as reported by ICP-MS is higher than the molar concentration of sulphate (SO_4^{2-}) as reported by Ion Chromatography. The same occurs for phosphorous (P) and phosphate (PO_4^{3-}). The PHREEQC simulations were conducted assuming that all sulphur is present as S(VI) (i.e. as sulphate: SO_4^{2-}), and assuming that all phosphorus (P) is present as P(V) (i.e. as phosphate: PO_4^{3-}), using the (higher) concentrations as obtained from ICP-MS;
4. As for the species that were already supersaturated in the feed (presented as phosphates, sulphates and carbonates), the arbitrary assumption was made that these compounds will already have precipitated, before entering the NF module. Consequently, concentrations of relevant elements (including Ca^{2+}, Mg^{2+}, and Ba^{2+}, and phosphate, sulphate and bicarbonate) were modified, by setting the saturation indices (SI) of those compounds to SI = 0,0 and subtracting the amount of apparently precipitated ions from the NF feed flow (04). Thus, the feed solution used as input for PHREEQC simulations was in saturated but not in supersaturated state;

Considering the four basic assumptions above, the feed solution for the NF process was defined as presented in Table 2, with an overall composition slightly different than that obtained from the actual samples.

For the flows 04, 06, 07, 08 and 10 (as indicated in Fig. 2), the ion product (IP) of different minerals was calculated, as well as the SI (Saturation Index), according to equation (1) below:

$$SI = \log(IP) + pK_{sp} \quad \text{eq. 1}$$

In this equation, pK_{sp} is the –log of the solubility product as provided by the PHREEQC database. When SI = 0, the solution is saturated. When SI < 0, saturation has not yet been reached, and when SI > 0, a supersaturated solution is observed, and salt is expected to precipitate until SI = 0 again. However, minerals will not immediately precipitate from a supersaturated solution, and very small (colloidal) particles may be present, without precipitation occurring. Thus, solutions with $0 < SI \leq 0.1$ are considered to be in a subsaturated state as well, and not considered to produce precipitation.

The amount actually leaving the system after precipitating may be difficult to calculate as the possibility to separate solids and remove them from the system depends on crystal size. This is especially so for salts with a very low solubility, which may produce extremely small crystals (colloids), as nucleation speed depends stronger on the SI than the speed of crystal growth, favoring the formation of huge amounts of very small crystals already at a very small supersaturation. In order to obtain larger and more handleable crystals, seeding is often applied, in which small crystals are provided to the mother liquor.

In the simulations, variations of process operating conditions like reject and permeate flows, operating pH, and temperature were

Table 1
Assumptions made regarding NF performance.

	Sample 1		Sample 2	
Recovery	70%		70%	
anion rejection (monovalent/multivalent)	46%	80%	46%	80%
cation rejection (monovalent/multivalent)	30%	60%	30%	50%

Table 2
NF feed solution as assumed for the simulations. The composition of this feed solution for the NF process as used for modeling the process differed slightly from the average composition of the spent IEX regenerant as obtained from sample analyses, given the need for a net zero charge.

cations and anions present		sample 1	sample 2
		mmol L^{-1}	mmol L^{-1}
Barium	Ba^{2+}	$1.58 .10^{-3}$	$6.86 .10^{-3}$
Calcium	Ca^{2+}	189	167
Cromium	Cr^{3+}	$1.68 .10^{-3}$	$2.78 .10^{-4}$
Copper	Cu^{2+}	0	$5.51 .10^{-4}$
Iron	Fe^{3+}	0.442	$5.74 .10^{-3}$
Potassium	K^{+}	5.39	6.22
Lithium	Li^{+}	$2.12 .10^{-2}$	$1.77 .10^{-2}$
Magnesium	Mg^{2+}	58.0	52.8
Manganese	Mn^{2+}	$1.05 .10^{-2}$	0
Sodium	Na^{+}	368	103
Nickel	Ni^{2+}	$2.24 .10^{-2}$	$3.60 .10^{-3}$
Lead	Pb^{2+}	$2.90 .10^{-4}$	0
Strontium	Sr^{2+}	0.503	0.352
Tellurium	Tl^{2+}	$1.45 .10^{-3}$	0
Vanadium	V^{5+}	$1.76 .10^{-2}$	$1.76 .10^{-3}$
Zinc	Zn^{2+}	0	$1.58 .10^{-3}$
Alkalinity	HCO_3^-	2.41	1.59
Chloride	Cl^-	851	557
Sulphate	SO_4^{2-}	9.26	1.58
Phosphate	PO_4^{3-}	$2.35 .10^{-3}$	$1.31 .10^{-4}$
pH		5.71	6.38

tested in order to optimize the process with regard to maximizing Mg and Ca salt production and minimizing secondary pollutant levels in the IEX regenerant solution. NF performance is an important parameter. In the first step, the spent IEX regenerant will be subjected to nanofiltration, which tends to reject polyvalent ions and permit passage of monovalent ions. Thus the reject will be enriched in ions like Ca^{2+} and Mg^{2+}, whilst the permeate will be enriched in monovalent ions like Na^{+} and K^{+}. To simulate the reject- and permeate flows of the NF unit, the following two assumptions were made:

1. The overall recovery of the NF process was assumed to be 70%, based on results from lab-scale experiments by the supplier of the NF unit, and corresponding to the membrane foreseen to be used. This recovery corresponds to various salinity levels of the feed as well, regardless the impact of module configuration;
2. It was assumed that the NF membranes used are typical NF membranes meaning negatively charged in an aqueous environment. Therefore, and confirmed by ongoing laboratory tests with membranes likely to be used in the pilot setup, rejection of multivalent-anions was considered to be 80%, and rejection of multivalent cations slightly less, decreasing with feed concentration. The rejection of monovalent anions was then adjusted in order to maintain charge conservation and avoid a negatively charged permeate and a positively charged reject (see Table 1).

Almost inevitably, the concentrate flow will contain combinations of ions that will exceed their solubility products. In practice, this may lead to scaling of the membrane, if the (unknown) residence time in the membrane module is long enough. For the PHREEQC simulations, this problem was dealt with by considering precipitation of the species with the highest SI value. Given the fact that most of the potentially supersaturated species contain Ca^{2+} and Mg^{2+}, this also means a potential loss of target mass, and a lower recovery of the target compounds in the subsequent crystallization processes. Location and effects of any precipitation of salts in the NF unit were disregarded though, as, within the scope of this project, it is not possible to foresee what exactly will happen inside the NF modules. The use of antiscalants to avoid precipitation and scaling was not considered during calculations as (i) the effect of these compounds on solubility products cannot be modeled adequately using PHREEQC, and (ii) the actual use of such compounds in a system with a closed loop water cycle will result in an undesirable accumulation of these compounds in the cycle; and should thus be avoided as much as possible.

After calculating the permeate and reject flows from NF, the recovery of magnesium and calcium in the crystallization units, as their respective hydroxides, was calculated. For this purpose:

1. In two separate crystallization units (D and E in Fig. 2), sodium hydroxide (NaOH) is injected ("Required Chemical" in the scheme). As informed by the supplier of the crystallization units, the amount of injected NaOH is calculated via a stoichiometric approach. That is, to precipitate 1 mol of either magnesium or calcium, 2 mol of NaOH are injected;
2. To quantify the amount of salts that can be recovered, a PHREEQC simulation was conducted in which the SI value of brucite ($Mg(OH)_2$) or portlandite ($Ca(OH)_2$) was simply set to a value of 0.0. The calculated concentration of Mg^{2+} and Ca^{2+} for these situations can then be subtracted from the concentration entering the process unit, giving the amounts expected to precipitate.

As for the evaporator unit simulation, two scenarios were considered: first, only the NF permeate (flow 06) as the input to the evaporator unit; and second, a mix of NF permeate (flow 06) and crystallizer supernatant (flow 10) as the input. For both scenarios, the overall recovery of distilled water from the evaporator unit was assumed to be 42%, i.e. 58% water remaining as NaCl brine (flow 13) which should then be suitable for reuse as IEX regenerant. Based on this, ion concentrations were recalculated and put into PHREEQC to estimate if there is a potential scaling problem. A preliminary estimation of these two types of feed was conducted to check if some species were supersaturated, and if so, SI values of supersaturated species were set to 0.0 to ensure no specie exceeded its solubility in the evaporator input.

A schematic representation of the modeling approach is presented in Fig. 3 below:

3. Results and discussion

3.1. Composition of the analyzed samples

Two series of measurements were obtained for spent IEX regenerant, as shown in Table 3 and Fig. 4. The major cations present in the samples are: Na^{+}, Ca^{2+}, and Mg^{2+}. The concentration of Ca^{2+} is around 3.5 times the concentration of Mg^{2+}, with the ratio between Na^{+} and the bivalent cations depending on the stage of the regeneration process. Also, lower concentrations of potassium (K^{+}), as well as minor concentrations (<0.1%) of other metals, most notably, strontium (Sr^{2+}), iron (Fe^{3+}) and barium (Ba^{2+}) were found. Trace amounts of elements like arsenic (As^{5+}), boron (B^{3+}), manganese (Mn^{4+}), copper (Cu^{2+}), zinc (Zn^{2+}) and cadmium (Cd^{2+}) are present in sample 1 but not in sample 2, whereas sample 2 contains around 100 times more iron (Fe^{3+}) and manganese (Mn^{2+}) then sample 1. Chloride (Cl^{-}) is the most abundant anion (>96%), next to much lower concentrations of bicarbonate (HCO_3^{-}), sulphate (SO_4^{2-}), and phosphate (PO_4^{3-}).

As elements were measured using ICP-MS, their oxidation state in the samples is not confirmed. Given the origin of the raw water and the processes involved, elements were assumed to be present in the oxidation state predominant in aerobic aqueous environments, as indicated.

As discussed above, samples 1 and 2 differed significantly. However, without additional data, it is arbitrary to attribute the variations in concentrations of each element to seasonal effects, as operational conditions, for example the time of use of the IEX resin and the amount of water used during the regeneration process may also lead to different compositions of spent regenerants. The fact that for both samples the calculated TDS concentration (sum of weights of identified anions and cations) is slightly higher than the TDS concentration measured by gravimetry confirms that no or very little additional (organic) reagents (coagulants, flocculants, anti-scaling agents etc.) were present in the samples, as these would increase the measured TDS but not the calculated TDS.

After obtaining these results a problem was detected, as several combinations of ions (most notably involving Ca^{2+}, Ba^{2+}, CO_3^{2-} and SO_4^{2-}) result in solubility products being exceeded. Preliminary PHREEQC simulations showed that species that may precipitate in the NF module (SI > 0.1) are different between the samples. Not all predicted precipitations however are relevant. In sample 2 for instance, magnetite (Fe_3O_4) exhibits the highest scaling potential (SI = 23.75) but at a concentration level of <1 μg L^{-1}. When considering only species with precipitation potentials above 1 μg L^{-1} levels, eight species remain, of which the SI values are generally below 2.00 (Table 4). In sample 1, in total 24 species are supersaturated, amongst which five species with SI values > 10. In this case again, Fe is the most sensitive element, due to its low solubility in the water matrix. In practice though, only eight species are capable of precipitating more than 1 μg L^{-1}, and only three species will actually precipitate from both samples More detailed information can be found in Table 4. As can be seen, only very small amounts of minerals (in general: sulphates or carbonates) are expected to precipitate:

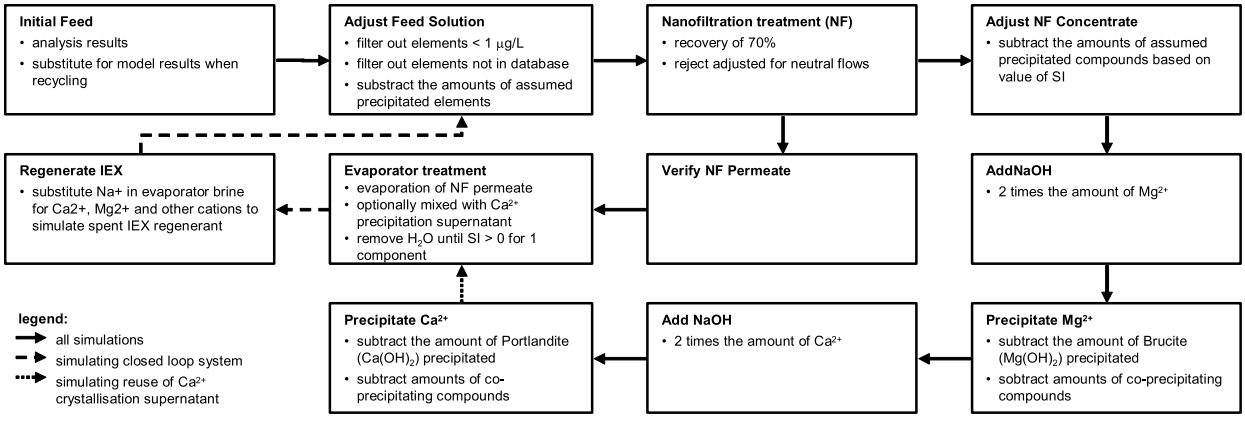

Fig. 3. Flowchart of the modeling approach.

Table 3
Results of analysis of two samples of spent IEX regenerant. Concentrations in mM. To obtain concentrations in mg L^{-1}, multiply by molar weight (MW).

Cations		MW	conc.[1,2] (mmol L^{-1})		Anions		MW	conc.[2] (mmol L^{-1})	
		g mol^{-1}	sample 1	sample 2			g mol^{-1}	sample 1	sample 2
Aluminium	Al^{3+}	27.0	0.000 072	< DL	Chloride	Cl^-	35.5	528.99	808.78
Antimony	Sb^{5+}	121.8	0.000 004	0.000 081	Fluoride	F^-	19.0	< DL	< DL
Barium	Ba^{2+}	137.8	0.025 9	0.036 1	Bromide	Br^-	79.9	< DL	< DL
Beryllium	Be^{2+}	9.0	< DL	< DL	Nitrite	NO_2^-	46.0	< DL	< DL
Cadmium	Cd^{2+}	112.4	0.000 002	< DL	Nitrate	NO_3^-	62.0	–	–
Calcium	Ca^{2+}	40.1	162.63	206.40	Phosphate	PO_4^{3-}	95.0	0.02	0.3
Cobalt	Co^{2+}	58.9	< DL	0.000 469	Sulphate	SO_4^{2-}	96.1	1.55	34.1
Copper	Cu^{2+}	63.5	0.000 53	< DL	Silicate	SiO_4^{4-}	92.1	0.03	< DL
Chromium	Cr^{3+}	52	0.000 27	0.001 59	Bicarbonate	HCO_3^-	61.0	2.34	2.29
Iron	Fe^{3+}	55.8	0.005 56	0.420					
Lead	Pb^{2+}	207.2	< DL	0.000 28					
Lithium	Li^+	6.9	0.017 1	0.020 2					
Manganese	Mn^{2+}	54.9	0.000 26	0.01					
Magnesium	Mg^{2+}	24.3	51.28	55.15					
Molybdenum	Mo^{4+}	95.9	0.000 015	0.000 14					
Nickel	Ni^{2+}	58.7	0.003 5	0.021 3					
Potassium	K^+	39.1	6.03	5.12					
Silver	Ag^+	107.9	< DL	0.000 018					
Sodium	Na^+	23.0	99.96	349.49					
Strontium	Sr^{2+}	87.6	0.342	0.478					
Titanium	Ti^{2+}	47.9	0.000 002	0.001 35					
Thallium	Tl^{3+}	208.4	< DL	< DL					
Vanadium	V^{5+}	50.9	0.001 7	0.016 7					
Zinc	Zn^{2+}	65.4	0.001 5	< DL					
Total Dissolved Solids (TDS)[3]			**29 382**	**50 038**	mg L^{-1}		pH	7.26	7.10
			29 139	*46 176*	mg L^{-1}				

1: for simulations, all elements assumed to be present in the form of the ion most abundant in aerated surface water, as listed; 2: < DL: below detection limit (generally <1 μg L^{-1}), 3: TDS, **as sum of all ions** (calculated) and *as measured*.

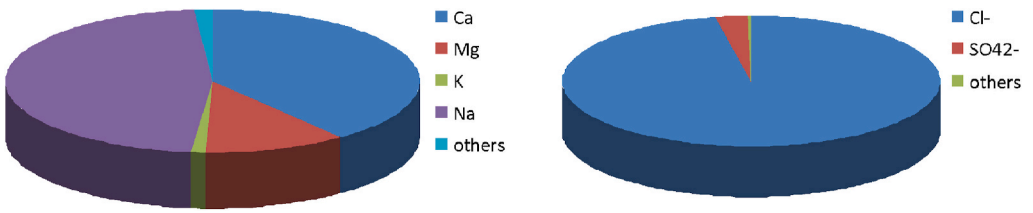

Fig. 4. Composition of spent IEX regenerant in terms of cations (left) and anions (right). Bivalent cations Ca^{2+} and Mg^{2+} are major constituents and may be recovered.

Table 4
Saturation Indexes (SI) of mineral species relevant for samples 1 and 2 (selection of SI > 0.1), and amounts precipitated (subtracted) to obtain a non-supersaturated NF feed solution.

Mineral Specie	Formula	Sample 1		Sample 2	
		SI	precipitated (mg L^{-1})	SI	precipitated (mg L^{-1})
Anhydrite	$CaSO_4$			0.61	0.026 6
Aragonite	$CaCO_3$	0.91		0.94	
Barite	$BaSO_4$	0.61	0.000 019 8	1.95	0.000 036 4
Calcite	$CaCO_3$	1.05	0.000 36	1.07	
Dolomite	$CaMg(CO_3)_2$	1.71		1.70	
Gypsum	$CaSO_4{\cdot}2H_2O$			0.56	
Hydroxyapatite	$Ca_5(PO_4)_3OH$	12.02	0.000 018 9	15.96	0.000 324
Magnesite	$MgCO_3$	0.16		0.13	

3.2. PHREEQC modeling results

3.2.1. NF concentrate composition

For each sample, based on the assumptions made regarding recovery and anion and cation reject, as well as the mass balance, the

concentration of each element can be calculated for each stream (concentrate and permeate). A summary of concentrate quality of the two samples is shown in Table 5.

As a result of concentrating the ions present in the feed in a smaller volume of concentrate, for some species the solubility product may be exceeded, resulting in a supersaturated solution, subject to precipitation. The value of the saturation index (SI, eq. (1)), shown in Table 4, indicates if this is expected to be the case. However, the effect is only relevant if not only the SI exceeds a minimum value, but also the amount of material available for precipitation is significant. Some ions are present in such low concentrations that the amount that might precipitate would be only in the order of micrograms per liter. Species that both have a saturation index SI > 0.1 and a concentration level of mg L^{-1} (rather than μg L^{-1}) are listed in Table 6.

In the case of sample 2, four species will become supersaturated in the NF concentrate stream, with hydroxyapatite being the most saturated (SI = 2.94). For sample 1, the number of supersaturated species is five, with again hydroxyapatite being the most supersaturated compound, with SI = 10.53. As the amount of hydroxyapatite precipitating is very small though, the most serious scaling might actually occur by precipitation of aragonite in sample 1 or anhydrite in sample 2, the latter as a result of the higher sulphate concentration in that sample. In this last case, it can be argued that gypsum rather than anhydrite will precipitate [11], but as the solubility products of both salts are of the same order of magnitude, we accepted the outcome of PHREEQC calculations in which anhydrite precipitates first. Regardless, the practical implications of precipitating either anhydrite of gypsum in terms of removal of ions from solution and amount (mass) of solids precipitated in the system will be roughly the same, and the beforementioned paper also shows that at increased salinity gypsum precipitation is reduced in favor of anhydrite and bassanite precipitation [11].

It can be seen that some 5% of calcium would precipitate as a result of the presence of sulphate in sample 2, which would cause scaling of process equipment. This means the NF process may experience more severe calcium scaling when fed with sample 2. Because most of the potentially supersaturated species contain Ca^{2+} and Mg^{2+}, this also means a potential loss of target mass, and lower recovery of the target compounds in the subsequent crystallization processes.

3.2.2. Salt recovery: amounts and purity

Table 7 presents the amounts of brucite and portlandite that are supposed to be recovered and their respective purities. The overall recovery of Ca and Mg for each liter of spent IEX regenerant fed to the NF is listed in Table 8. Results for both samples are consistent, both suggest that more than 50% of the amount of target salts can be recovered, and with high quality, especially for calcium, with more than 97% purity for both samples.

Some low-solubility species (listed in Table 9) may be co-precipitated when the SI of such a compound has a value of SI > 0. This may occur especially in the first crystallizer (D), intended for magnesium recovery, resulting in a slightly lower purity of magnesium. Still Mg^{2+} will be of 96.4% purity even in the worst case (sample 2), with $Ca(OH)_2$ and $CaCO_3$ the major pollutants (1.8% each of the precipitate in moles). In the second crystallizer, the situation is inverted: now $Ca(OH)_2$ is the predominant material, and $Mg(OH)_2$ is the main impurity, but in this case the best quality product is obtained from sample 2 (99,1% purity) and a lesser quality product obtained from sample 1 (97.4% purity, with $Mg(OH)_2$ the main pollutant). More detailed information can be found in Table 8.

The effect of running the process under conditions of different temperature and pH were not calculated as not deemed very relevant. As can be seen in Fig. 1, solubilities of key precipitates brucite and portlandite hardly vary in the range of temperatures of 10–35 ˚C (and lower temperatures negatively affect membrane filtration, where higher temperatures incur costs of heating large volumes of dilute solutions), making it likely that the process will be run at available water temperature. The effect of altering the pH

Table 5
Composition of NF concentrates (feed for Mg-crystallization unit) at 70% recovery.

ions present		sample 1			sample 2		
		mg L^{-1}	mol L^{-1}	precip. (mg L^{-1})	mg L^{-1}	mol L^{-1}	precip. (mg L^{-1})
Barium	Ba^{2+}	2.18	$1.49 .10^{-5}$	1.40	0.58	$3.79 .10^{-6}$	
Calcium	Ca^{2+}	15 487	$3.62 .10^{-1}$	12.8	20 257	$4.54 .10^{-1}$	954
Cromium	Cr^{3+}	0.03	$6.02 .10^{-7}$		0.23	$4.03 .10^{-6}$	
Copper	Cu^{2+}	0.08	$1.19 .10^{-6}$				
Iron	Fe^{3+}	0.74	$1.24 .10^{-5}$		65.9	$1.06 .10^{-3}$	
Potassium	K^{+}	442	$1.06 .10^{-2}$		399	$9.16 .10^{-3}$	
Lithium	Li^{+}	0.22	$3.01 .10^{-5}$		0.28	$3.60 .10^{-5}$	
Magnesium	Mg^{2+}	2958	$1.14 .10^{-1}$		3761	$1.39 .10^{-1}$	
Manganese	Mn^{2+}				1.54	$2.52 .10^{-5}$	
Sodium	Na^{+}	4295	$1.75 .10^{-1}$		16 022	$6.26 .10^{-1}$	
Nickel	Ni^{2+}	0.49	$7.80 .10^{-6}$		3.52	$5.38 .10^{-5}$	
Lead	Pb^{2+}				0.16	$6.96 .10^{-7}$	
Strontium	Sr^{2+}	71.4	$7.63 .10^{-4}$		118	$1.21 .10^{-3}$	
Tellurium	Tl^{2+}				0.81	$3.48 .10^{-6}$	
Vanadium	V^{5+}	0.21	$3.81 .10^{-6}$		2.39	$4.22 .10^{-5}$	
Zinc	Zn^{2+}	0.24	$3.42 .10^{-6}$				
Bicarbonate	HCO_3^-	215	$3.30 .10^{-3}$	19.7	340	$5.00 .10^{-3}$	
Chloride	Cl^-	43 580	1.15		69 559	1.76	
Sulphate	SO_4^{2-}	464	$4.53 .10^{-3}$	0.980	2832	$2.65 .10^{-2}$	2290
Phosphate	PO_4^{3-}	0.04	$3.76 .10^{-7}$	0.0137	0.71	$6.74 .10^{-6}$	0.635

Table 6
Scaling potential of NF concentrate, considering operating conditions as defined in Table 1. The risk of scaling depends mainly on anion concentrations in the sample.

Mineral specie	Formula	Sample 1		Sample 2	
		SI	precipitated (mg L^{-1})	SI	precipitated (mg L^{-1})
Anhydrite	$CaSO_4$			0.72	3290
Aragonite	$CaCO_3$	0.51	32.7		
Barite	$BaSO_4$	1.05	2.38	0.45	
Calcite	$CaCO_3$	0.65			
Dolomite	$CaMg(CO_3)_2$	0.94			
Gypsum	$CaSO_4{\cdot}2H_2O$			0.65	
Hydroxyapatite	$Ca_5(PO_4)_3OH$	10.53	0.0723	2.94	3.36
Magnesite	$MgCO_3$				

Table 7
Amount of recovered salts (g L^{-1}) of NF feed in crystallizers D (Mg-crystallizer) and E (Ca-crystallizer).

Species		Mg crystallizer (D)		Ca-crystallizer (E)	
		Sample 1	Sample 2	Sample 1	Sample 2
Barite	$BaSO_4$	0.000 20			
Brucite	$Mg(OH)_2$	6.52	8.75	0.54	0.23
Calcite	$CaCO_3$	0.32	0.56		
Hydroxyapatite	$Ca_5(PO_4)_3OH$	0.000 04	0.00014		
Portlandite	$Ca(OH)_2$			25.80	32.91
Purity (mass fraction)		95%	94%	98%	99%

Table 8
Recovery of Mg and Ca as their hydroxides and as other salts.

Recovered ions	Sample 1		Sample 2	
	Mg-crystallizer	Ca-crystallizer	Mg-crystallizer	Ca-crystallizer
Mg^{2+}, as $Mg(OH)_2$	60.0%	4.98%	70.2%	1.82%
Mg^{2+}, as other minerals				
Ca^{2+}, as $Ca(OH)_2$		58.6%		63.4%
Ca^{2+}, as other minerals	0.54%		0.79%	

Table 9
Saturation Indices (SI) of minerals during salt recovery steps (omitted when SI < 0).

Species		Mg recovery		Ca recovery	
		Sample 1	Sample 2	Sample 1	Sample 2
Aragonite	$CaCO_3$	2.75	3.03		
Artinite	$MgCO_3{\cdot}Mg(OH)_2{\cdot}3H_2O$	6.88	7.21	2.30	1.31
Barite	$BaSO_4$	0.11			
Brucite	$Mg(OH)_2$	6.10	6.21	6.11	5.79
Calcite	$CaCO_3$	2.89	3.17		
Dolomite	$CaMg(CO_3)_2$	4.99	5.54		
Huntite	$CaMg_3(CO_3)_4$	5.12	6.18		
Hydromagnesite	$Mg_5(CO_3)_4(OH)_2{\cdot}4H_2O$	5.97	7.07		
Hydroxyapatite	$Ca_5(PO_4)_3OH$	14.58	16.37	2.62	2.25
Magnesite	$MgCO_3$	1.61	1.87		
Periclase	MgO	1.45	1.58	1.47	1.16
Portlandite	$Ca(OH)_2$	1.10	1.24	2.60	2.77

was not studied as adding any additional amount of base will increase precipitation of species later on, increasing impurities in the product, whereas dosing less hydroxide, or adding acid to decrease the amount of hydroxide ions, will reduce the amount of minerals precipitated. Hydroxide dosing in the crystallization reactors will need to be done stoichiometrically, considering the amounts of cations to be precipitated rather than aiming at a specific pH.

3.2.3. Evaporator: feed and product

To close the water cycle, an evaporation step was foreseen, which produces distilled (pure) water and a brine (containing

predominantly sodium chloride, NaCl). This evaporation step, as mentioned before, can be fed in two ways: besides receiving only the NF permeate, a mix of NF permeate and the crystallizer effluent can also be defined as the input to the evaporator. A summary of the composition of the two mixed feeds is listed in Table 10.

Since 42% of the water will be evaporated, a concentrated solution will be obtained. Table 11 presents an estimation of the composition of this concentrated solution, for both situations: feeding the evaporator only with the NF permeate, or feeding the evaporator with a mix of NF permeate and crystallization supernatant. For both samples, sodium and chloride are the dominant cation and anion respectively. Ca^{2+} is the second most abundant cation in the product, with 3% (sample 2) or 6% (sample 1) of the total cation concentration. When using only the NF permeate as feed, these percentages actually become slightly higher. Thus, alternatives for reusing this brine for IEX regeneration have to be studied. When it comes to the foreseeable scaling in the evaporator, if NF permeate is the only influent no scaling will be detected for either sample. However, when using the mixed feed, the situation is different. Some species will become supersaturated in the evaporator (see Table 12), and consequently, scaling becomes a possibility. In this respect, the presence of calcium is the main risk factor regarding this possible scaling problem in the evaporator unit.

4. Conclusions

Magnesium and calcium may be separated with efficiently from spent IEX regenerant, however complete (>99%) recovery of these materials is not possible. Especially in the case of calcium, a small part of the material can also end up as scaling before reaching the crystallization step.

Although theoretically selective precipitation of Mg(OH)2 and Ca(OH)2 is possible, producing them in pure form is almost impossible, because together with these hydroxides, depending on the anions present, also carbonates, sulphates and other minerals may co-precipitate. Given the widely varying concentrations of anions found in the different samples, the amount of impurities in the precipitates will vary, but precipitates will contain Mg and Ca with at least 97% purity in all cases studied.

The amount of hydroxides recovered is directly dependent on the amount of hydroxide dosed. Hydroxide dosing should therefore be carefully controlled as, especially in the first crystallization reactor, excess NaOH dosed might cause $Ca(OH)_2$ to precipitate prematurely. Control of hydroxide dosing for Mg^{2+} and Ca^{2+} precipitation can most likely be based on supernatant pH, as in the case of correct stoichiometric dosing, this pH will be around 9.7 and 12.5 after Mg^{2+} and Ca^{2+} precipitation, respectively, for both samples, practically independent of initial metal ion concentration.

Evaporator performance depends greatly on the feed. If only NF permeate is fed, no scaling occurs at the evaporator unit, while when feeding a mixture of NF permeate and crystallization supernatant, calcium scaling may occur there. In the same way, when feeding only NF permeate, the quality of the brine produced, with respect to the abundance of sodium and chlorine ions, is higher than when compared to the situation that a mixture of NF permeate and crystallizer effluent is fed to the evaporator. When using this mixture as feed, the brine produced by the evaporator cannot be used for regeneration of the IEX columns, because in this case accumulating impurities will cause a faster exhausting of the IEX columns, a need for more frequent regeneration of these columns, more frequent replacement of the resin, and consequently higher operational and environmental costs. It will be essential to carefully

Table 10
Composition of evaporator feed solution, being either only NF permeate or a mixture of NF permeate with the crystallization supernatant. Most abundant cation and anion in bold.

		NF **Perm.** + Cryst. Effl.		NF Permeate	
		Sample 1	Sample 2	Sample 1	Sample 2
pH		12.15	12.16	6.37	
cations (mol L^{-1})					
Barium	Ba^{2+}	$4.42 .10^{-6}$	$3.15 .10^{-6}$	$3.50 .10^{-6}$	$6.49 .10^{-7}$
Calcium	Ca^{2+}	$5.04 .10^{-2}$	$4.52 .10^{-2}$	$\mathbf{8.79 .10^{-2}}$	$7.76 .10^{-2}$
Cromium	Cr^{3+}	$4.93 .10^{-7}$	$3.35 .10^{-6}$	$1.45 .10^{-7}$	$6.90 .10^{-7}$
Copper	Cu^{2+}	$9.76 .10^{-7}$		$2.89 .10^{-7}$	$1.82 .10^{-4}$
Iron	Fe^{3+}	$1.02 .10^{-5}$	$8.80 .10^{-4}$	$3.01 .10^{-6}$	$3.87 .10^{-3}$
Potassium	K^{+}	$9.29 .10^{-3}$	$8.30 .10^{-3}$	$4.57 .10^{-3}$	$1.52 .10^{-5}$
Lithium	Li^{+}	$2.64 .10^{-5}$	$3.26 .10^{-5}$	$1.30 .10^{-5}$	$2.38 .10^{-2}$
Magnesium	Mg^{2+}	$8.30 .10^{-3}$	$7.15 .10^{-3}$	$2.77 .10^{-2}$	$4.31 .10^{-6}$
Sodium	Na^{+}	$\mathbf{8.50 .10^{-1}}$	**1.45**	$7.57 .10^{-2}$	$\mathbf{2.65 .10^{-1}}$
Nickel	Ni^{2+}	$6.40 .10^{-6}$	$4.47 .10^{-5}$	$1.89 .10^{-6}$	$9.20 .10^{-6}$
Strontium	Sr^{2+}	$6.26 .10^{-4}$	$1.00 .10^{-3}$	$1.85 .10^{-4}$	$1.19 .10^{-7}$
Vanadium	V^{5+}	$3.12 .10^{-6}$	$3.51 .10^{-5}$	$9.24 .10^{-7}$	$2.06 .10^{-4}$
Zinc	Zn^{2+}	$2.80 .10^{-6}$		$8.29 .10^{-7}$	$5.96 .10^{-7}$
Manganese	Mn^{2+}		$2.09 .10^{-5}$		$4.20 .10^{-6}$
Lead	Pb^{2+}		$5.78 .10^{-7}$		$1.16 .10^{-7}$
Tellurium	Tl^{2+}		$2.89 .10^{-6}$		$5.80 .10^{-7}$
anions (mol L^{-1})					
Bicarbonate	HCO_3^-	$2.68 .10^{-4}$	$4.03 .10^{-4}$	$8.84 .10^{-4}$	$1.34 .10^{-3}$
Chloride	Cl^-	$\mathbf{9.54 .10^{-1}}$	**1.51**	$\mathbf{3.15 .10^{-1}}$	$\mathbf{4.72 .10^{-1}}$
Sulphate	SO_4^{2-}	$3.48 .10^{-3}$	$4.54 .10^{-3}$	$3.32 .10^{-4}$	$1.90 .10^{-3}$
Phosphate	PO_4^{3-}	$8.20 .10^{-9}$	$1.45 .10^{-7}$	$2.73 .10^{-8}$	$4.83 .10^{-7}$

Table 11
Composition of the brine produced after evaporation.

		NF **Perm.** + Cryst. Effl.		NF Permeate	
		Sample 1	Sample 2	Sample 1	Sample 2
pH		12.07	12.12		
cations (mol L^{-1})					
Sodium	Na^{+}	1.47	2.50	$4.57 .10^{-1}$	$1.31 .10^{-1}$
Calcium	Ca^{2+}	$8.64 .10^{-2}$	$7.72 .10^{--2}$	$1.34 .10^{-1}$	$1.52 .10^{-1}$
Potassium	K^{+}	$1.60 .10^{-2}$	$1.43 .10^{-2}$	$6.68 .10^{-3}$	$7.88 .10^{-3}$
Strontium	Sr^{2+}	$1.08 .10^{-3}$	$1.73 .10^{-3}$	$3.56 .10^{-4}$	$3.19 .10^{-4}$
Iron	Fe^{3+}	$1.75 .10^{-5}$	$1.52 .10^{-3}$	$3.13 .10^{-4}$	$5.19 .10^{-6}$
Nickel	Ni^{2+}	$1.10 .10^{-5}$	$7.71 .10^{-5}$	$1.59 .10^{-5}$	$3.26 .10^{-6}$
Vanadium	V^{5+}	$5.39 .10^{-6}$	$6.05 .10^{-5}$	$1.25 .10^{-5}$	$1.59 .10^{-6}$
Lithium	Li^{+}	$4.55 .10^{-5}$	$5.63 .10^{-5}$	$2.62 .10^{-5}$	$2.25 .10^{-5}$
Manganese	Mn^{2+}		$3.61 .10^{-5}$	$7.44 .10^{-6}$	
Cromium	Cr^{3+}	$8.51 .10^{-7}$	$5.77 .10^{-6}$	$1.19 .10^{-6}$	$2.51 .10^{-7}$
Barium	Ba^{2+}	$4.82 .10^{-6}$	$5.43 .10^{-6}$	$1.12 .10^{-6}$	$6.03 .10^{-6}$
Tellurium	Tl^{2+}		$4.99 .10^{-}$	$1.03 .10^{-6}$	
Lead	Pb^{2+}		$9.97 .10^{-7}$	$2.05 .10^{-7}$	
Magnesium	Mg^{2+}	$8.73 .10^{-7}$	$6.70 .10^{-7}$	$4.11 .10^{-2}$	$4.77 .10^{-2}$
Copper	Cu^{2+}	$1.68 .10^{-6}$			$4.98 .10^{-7}$
Zinc	Zn^{2+}	$4.84 .10^{-6}$			$1.43 .10^{-6}$
anions (mol L^{-1})					
Bicarbonate	HCO_3^-	1.65	2.61	$4.77 .10^{-2}$	$1.52 .10^{-3}$
Sulphate	SO_4^{2-}	$5.99 .10^{-3}$	$7.85 .10^{-3}$	$3.28 .10^{-3}$	$5.72 .10^{-4}$
Chloride	Cl^-	$1.61 .10^{-5}$	$2.24 .10^{-5}$	$8.15 .10^{-1}$	$5.44 .10^{-1}$
Phosphate	PO_4^{3-}	$2.63 .10^{-11}$	$2.67 .10^{-11}$	$8.32 .10^{-7}$	$4.70 .10^{-8}$

Table 12
Amounts of species possibly precipitating during evaporation (mol L^{-1}).

Species		NF **Perm.** + Cryst. Effl.		NF Permeate	
		Sample 1	Sample 2	Sample 1	Sample 2
Barite	$BaSO_4$	$8.55 .10^{-7}$	$1.05 .10^{-6}$	–	–
Brucite	$Mg(OH)_2$	$2.58 .10^{-7}$	$3.39 .10^{-7}$	–	–
Calcite	$CaCO_3$	$6.53 .10^{-6}$	$4.51 .10^{-6}$	–	–
Hydroxyapatite	$Ca_5(PO_4)_3OH$	$3.46 .10^{-12}$	$3.27 .10^{-12}$	–	–

study the crystallizer effluent, and consider other options before deciding on mixing this effluent with the NF permeate as the feed for the evaporator.

In spite of the great detail of the modeling results, the exact effect of closing the water cycle in the process cannot yet be calculated completely. In the first place because a large variation between samples (process cycle input) was observed, and in the second place because the exact process scheme and process control strategy have not yet been defined. Even with the limited amount of data, the modeling study shows that a completely closed cycle is not a realistic goal, and some type of bleed will need to be present. Without a bleed, all ions present in the feed but not removed as product, like for instance Ni^{2+}, Zn^{2+}, Sr^{2+} and nitrate, to name a few, will over time accumulate in the regeneration cycle, causing deterioration of the process and product specifications in the long run. Bleeding however may be as simple as releasing part of the mother liquor of Ca-precipitation; or releasing part of the NF permeate.

Author contributions

Conception and design of study: H. Spanjers, A. Haidari. Data aquisition and modeling: M.A. Boncz, N. van Linden, A. Haidari. Data analysis and interpretation: M.A. Boncz, N. van Linden, Y. Wang. Manuscript drafting: M.A. Boncz, N. van Linden, Y. Wang. Manuscript revision: M.A. Boncz, N. van Linden, Y. Wang, H. Spanjers.

Declaration of competing interest

The authors declare that they have no known competing financial interests or personal relationships that could have appeared to influence the work reported in this paper.

Acknowledgements

This project has received funding from the European Union's Horizon 2020 research and innovation programme under Grant Agreement no. 730390 (ZERO BRINE – Industrial Desalination – Resource Recovery – Circular Economy). www.zerobrine.eu.

References

[1] J. van Agtmaal, H. Huiting, P.A. de Boks, L.L.M.J. Paping, Four years of practical experience with an Integrated Membrane System (IMS) treating estuary water, Desalination 205 (1–3) (2007) 26–37, https://doi.org/10.1016/j.desal.2006.02.049.

[2] A.H. Haidari, B. Blankert, H. Timmer, S.G.J. Heijman, W.G.J. van der Meer, PURO: a unique RO-design for brackish groundwater treatment, Desalination 403 (2015) 208–216, https://doi.org/10.1016/j.desal.2015.09.015.

[3] T. Manth, J. Frenzel, A. van Vlerken, Large-scale application of UF and RO in the production of demineralized water, Desalination 118 (1–3) (1998) 255–262, https://doi.org/10.1016/S0011-9164(98)00140-4.

[4] A.W. Mohammad, R. Othaman, N. Hilal, Potential use of nanofiltration membranes in treatment of industrial wastewater from Ni-P electroless plating, Desalination 168 (15) (2004) 241–252, https://doi.org/10.1016/j.desal.2004.07.004.

[5] J.W. van der Merwe, Application of nanofiltration in metal recovery, J. S. Afr. Inst. Min. Metall 98 (7) (1998) 339–341, https://doi.org/10.10520/AJA0038223X_2491.

[6] R.S. Arvidson, F.T. Mackenzie, Tentative kinetic model for dolomite precipitation rate and its application to dolomite distribution, Aquat. Geochem. 2 (1997) 273–298, https://doi.org/10.1007/BF00119858.

[7] R.C. Weast, CRC Handbook of Chemistry and Physics, 73 ed., CRC Press Inc. 2489, Boca Raton, FLA, USA, 1993.

[8] D.L. Parkhurst, L. Wissmeier, PhreeqcRM: a reaction module for transport simulators based on the geochemical model PHREEQC, Adv. Water Resour. 83 (2015) 176–189, https://doi.org/10.1016/j.advwatres.2015.06.001.

[9] D.L. Parkhurst, C.A.J. Appelo, Description of input and examples for PHREEQC version 3—a computer program for speciation, batch-reaction, one-dimensional transport, and inverse geochemical calculations, in: Modeling Techniques, U.S. Geological Survey: Denver - CO, USA, 2013, p. 519.

[10] S.R. Charlton, D.L. Parkhurst, Modules based on the geochemical model PHREEQC for use in scripting and programming languages, Comput. Geosci. 37 (10) (2011) 1653–1663, https://doi.org/10.1016/j.cageo.2011.02.005.

[11] M. Ossorio, A.E.S. van Driessche, P. Pérez, J.M. García-Ruiz, The gypsum–anhydrite paradox revisited, Chem. Geol. 386 (2014) 16–21, https://doi.org/10.1016/j.chemgeo.2014.07.026.